Economic Assessment of Tidal Hydrokinetic Turbines Under Different Energy System Configurations

Loris Bigatton*[a], Victor Dachet[a], Damien Ernst[a], and Raphaël Fonteneau[a]

[a]Department of Electrical Engineering and Computer Science, ULiège, Liège, Belgium

Abstract

This article proposes a methodology to estimate the cost of electricity in energy systems where tidal hydrokinetic turbines (HKT) are used to harness tidal power. This cost is assessed for three different energy systems: (i) an off-grid island (i.e., without the possibility of consuming electricity from the mainland grid) where a local electricity demands need to be served from local renewable energy sources (HKT and other renewable energy sources), (ii) an on-grid industry interested in minimising its overall electricity bill by valorising renewable energy sources (HKT and other renewable energy sources), (iii) an electricity producer interested in maximising profit using HKT and selling electricity on the day-ahead market. In each of the three systems, battery storage may be installed. In our studies, investments in the different energy systems are optimised to minimise annual costs. The optimisation procedure relies on a linear program formulation. The optimisation results allow us to identify not only the costs but also the optimal capacity to install, as well as the best operational strategies regarding the time series used for the optimisation. Those are generated for different WACCs (Weighted Average Cost of Capital) and discussed. Our results show that there is a financial interest in investing in HKT when an electricity demand has to be served locally (energy systems (i) and (ii)). However, using this technology only for selling electricity to the wholesale market is not yet profitable (energy system (iii)).

Keywords: Energy systems, Optimisation, Hydrokinetic energy, Marine energy
***Corresponding author.** *E-mail address:* loris.bigatton@student.uliege.be (Loris Bigatton)

1 Introduction

Since the early 2000s, the threats caused by greenhouse gas (GHG) emissions [1] have led to the development of energy policies that have spurred the growth of renewable energy production [2]. This development has had a remarkable impact on the costs of renewable technologies such as solar PV and wind turbines. As a result, they have now become cheap sources of electricity [3, 4]. Nevertheless, two main issues appear with the development of these energy sources. The first relates to the opposition to building renewable energy infrastructures, such as wind farms, in many parts of the world. For example, a study in the US shows that renewable energy projects face socio-political barriers [5]. The authors also demonstrate that both the cultural and financial values of land need to be considered in the siting of renewable energy facilities. Additionally, reference [6] that analyses the opposition to renewable energy sources in the Nordic countries has shown that local conflicts, caused by renewable energy projects are multifaceted and driven by concerns over environmental impacts, visual disruption, distrust in regulatory processes, inadequate financial compensation, threats to cultural heritage, health risks, and social stress. In the windy UK, the specific case of wind turbines has been studied; field studies show that the more a project is visible and perceived to spoil the landscape, the lower the endorsement it receives [7]. The second one is the dependence of solar PV and wind turbines on meteorological conditions, such as sun or wind. This dependence complicates energy production forecasting, especially e.g., in parts of Europe which are subject to constant fluctuations in weather conditions, which may significantly challenge the operation of power systems [8, 9]. Additionally, this dependence on meteorological conditions may be associated with the *dunkelflaute* phenomena, representing large time windows with low production levels of renewables [10]. Power systems may be critically challenged during those time windows [11]. These problems justify the interest in studying other renewable sources whose production levels could be predicted more accurately, and which are not plagued by long periods of low production. Tidal hydrokinetic energy, which involves harnessing the energy of tides, is certainly one of such sources that could be worthwhile implementing in coastal areas. Indeed, tidal hydrokinetic energy is a predictable and regular source of energy, with only minor dependence on meteorological conditions, that could be used to generate electricity [12]. The minor dependence on weather conditions arises from the fact that near coastal areas, water flows can also be influenced by rainfall and river discharge, and so cannot be determined solely by tides. In this paper, we examine the economics of three electrical energy systems based on hydrokinetic turbines (HKT): the first involves two different configurations, which are detailed later, where the electricity demand of an island disconnected from the mainland's grid must be met, relying solely on local renewable energy sources and possibly battery storage. The second one corresponds to the situation of a factory with a local electricity demand partially (or totally) covered by renewable energy and possibly battery storage placed behind the same meter connecting this factory to the main utility grid. As in the first energy system, two configurations are detailed and studied later. We also assume a limited budget for the installation of renewable energy facilities and batteries, as companies face when dealing with investments in energy systems. We emphasise here that, contrary to the first class of energy systems, interaction with the main utility grid is authorised, which offers opportunities for buying and selling electricity on the market. The last one corresponds to the situation of an electricity producer that can deploy HKT and possibly battery storage behind the same meter to valorise the generated electricity on the market, at a price given by the day-ahead market. For the same reason as in the second system, we assume a limited budget. Contrary to the first two energy systems, no electricity demand can be met locally. We believe that these three energy systems effectively cover the different possible valorisation schemes for HKT, even if we could not exclude other ones, such as, for example, HKT systems that would be used in remote areas to synthesise e-fuels that would be exported later on to load centres [13–15]. For studying these energy systems, we will rely on models to determine the optimal investments to be made to minimise the annual costs and maximise the revenues. The models are developed using the GBOML language [16], a modelling tool specifically designed to model and optimise integrated energy systems. Works using this tool have already been done, see for instance [17, 18]. Further explanation will be furnished in Section 3. For each of these energy systems, we will report the cost of electricity, the configuration in terms of installed capacities and the best operational strategies regarding the time series used for the optimisation. These data correspond to the optimised versions of the energy systems where investments have been made to minimise the yearly costs.

In the experiments, we will first assume a Weighted Average Cost of Capital (WACC) equal to 0%. We will also analyse the influence of the WACC by reporting results related to non-zero WACC and, more specifically, a WACC of 3.5%, 7% and 10%. The rest of this paper is organised as follows. In Section 2, we discuss existing works that relate, for most of them, to the economics of HKT-based systems. Section 3 presents the methodology used for the optimisation of energy systems from which the electricity cost will be derived. A presentation of the different energy systems is also provided, along with the assumptions related to each energy system. Section 4 reports and briefly discusses the results related to the first, second and third energy systems. Section 5 compares and discusses the results of the previous section. Finally, Section 6 summarises outcomes of the simulations and concludes this paper. An appendix, containing information on the parameters used in our models, such as technology costs, technology lifetime, capacity factors, electricity demands and electricity prices, can be found in Appendix A.

2 Related work

Hydrokinetic energy is receiving increasing attention from the scientific community [19], in particular, because of the regularity of the tide, potentially leading to a more regular electricity production level compared to other renewable energy sources. Many of the techno-economic studies related to HKT focus on islandic energy systems. In this respect, one could first mention reference [20], where a techno-economic assessment is presented for the specific case of Cozumel Island, located in the Mexican Caribbean. In this reference, sixteen sites are studied. They determine the best locations in the areas surrounding the island, the optimal HKT device and associated data such as installed capacities and costs. Almoghayer et al. [21] focus on the specific case of the Orkney islands, located in northern Scotland, which have an electrical connection with the mainland grid. The authors identify suitable sites and the optimal types of turbines associated with those sites. Based on the previous results, they demonstrate the potential of integrating tidal energy into an island's energy system. The Goto islands, located in Japan, were also studied to determine the benefits of installing a tidal-wind-solar system to balance better supply/demand as well as grid security [22]. Other works focus on the use of those HKT systems for producing electricity for mainland loads located in remote areas. Johnson and Pride [23] examine the case of Alaska, located in the USA, where river, ocean and tidal currents appear to be promising techniques to generate electricity in Alaska. Ileberi and Li [24] studied the introduction of hydrokinetic energy into a hybrid energy system made of solar PV, wind turbines, HKT and diesel generators for the specific case of a Nigerian river. The authors demonstrate that the optimisation results for a community in Nigeria show significant potential for generating hydrokinetic energy, which contributes 38% of the total generation to cover the demand. Khojasteh et al. [25] report on a study on the specific case of Iran, where renewable energy sources were studied with a focus on wave and tidal energy. The authors have shown that there are many energy hotspots with a high potential for marine energy development in the Caspian Sea, the Persian Gulf and the Gulf of Oman. Other works have sought to assess the benefit of HKT in areas where the hydrokinetic source of energy does not only come from the tides but also from river discharge. In this respect, it is worth mentioning Fouz et al. [26]. Authors have shown that river discharge may also combine with tides by studying the specific case of the Miño estuary located in Spain.

This paper differs from the works discussed above by studying and comparing the techno-economic aspects of HKT in different energy systems, each containing one or two energy configurations. For each configuration, the optimal installation and operational strategies are determined to minimise annual costs and maximise annual revenues when selling electricity is authorised.

3 Modelling & assumptions

3.1 Modelling

In our approach, we optimise the different energy systems by carrying out a joint optimisation of the operational strategy and the investments to minimise yearly costs and maximise annual revenues when selling electricity is authorised. We use GBOML (Graph-Based Optimisation Modelling Language) [16] to model every system. In GBOML, every model is built as a hypergraph made of nodes and hyperedges. Nodes typically represent electricity generation technologies as well as the grid and batteries. Hyperedges are used to model constraints between nodes, such as energy balance or budget constraints. The installation and maintenance costs of all technologies are expressed in the form of CAPEX (CAPital EXpenditure) and OPEX (OPerational EXpenditure). When an interaction with the mainland's grid is possible, prices from the day-ahead electricity market corresponding to the French bidding zone in 2019 are used. Parameters are provided in the appendix and can be found with the code on the GitHub repository created for this research.[1] The resulting models are Linear Programs that are solved using the GUROBI solver [27] to minimise the overall costs, also taking the revenues into account when it is possible to sell surplus electricity on the mainland's grid.

3.2 Assumptions & presentation of the first energy system

The first energy system relates to an isolated island. In this first energy system, the objective is to serve the local demand while minimising the annualised costs, i.e annualised CAPEX plus OPEX. The electricity generated locally must be either used or stored in batteries to be consumed later. Curtailment is authorised, which means that we can decide not to produce the maximum energy we could produce from renewable resources. Two configurations are considered: first, we consider a configuration relying on tidal energy only, and second, we allow the installation of other local renewable energy resources, namely HKT, solar PV and wind offshore turbines. In both configurations, the WACC is assumed to be equal to zero. The annualised CAPEX of a technology is computed by dividing the CAPEX of this technology by its lifetime. Batteries are allowed in both the first and second configurations. We assume that the demand of the island corresponds to the demand of approximately 1,200 inhabitants, with a consumption being equal to the average yearly consumption of a mainland France resident. The hourly average power demand of those inhabitants follows the hourly average power demand of France for 2019, as reported by RTE.[2] This power demand curve can be found in Figure 12 and a further explanation on how it was generated can be found in the appendix (Section A). The hydrokinetic turbine capacity factor depends on time and is approximately six hours periodic, as shown in Figure 9. The data are synthetic, since we have not had the chance yet to get access to measured data. A further explanation on how the data were generated can be found in Appendix A.

As HKT is a new source of energy compared to solar PV or wind turbines, its costs are uncertain. The 2022 OceanSET Third Annual Report [3] proposed costs and estimated lifetimes for three different years (2018, 2019 and 2020). We decided to use the lowest CAPEX (€3.4m/MW) and OPEX (€0.1m/MW/year) and the highest lifetime (22.5 years) to understand if HKT may be a potential energy source. We believe that, similar to solar PV and wind turbines [3, 4], HKT cost will further decrease in the future. We think that this reduction could be the result of economies of scale or technological advances. We will therefore study the impact of a potential reduction in HKT CAPEX and

[1] https://github.com/lorisbigatton/HKT-Economic-Assessments
[2] https://www.rte-france.com/eco2mix/telecharger-les-indicateurs
[3] https://www.oceanset.eu/wp-content/uploads/2022/03/OceanSET-Third-Annual-Report-March-2022.pdf

OPEX on installed capacities and expenses. Other parameters (electricity load, battery costs, capacity factors and lifetimes) remain the same. The evolution of the HKT CAPEX ($c_{\text{cap}}^{\text{HKT}}$) and OPEX ($c_{\text{op}}^{\text{HKT}}$) is formalised as follows:

$$c_{\text{cap}}^{\text{HKT}}(\lambda) = \frac{c_{\text{cap}}^{\text{HKT}}}{1 + 0.05\lambda} \tag{1}$$

$$c_{\text{op}}^{\text{HKT}}(\lambda) = \frac{c_{\text{op}}^{\text{HKT}}}{1 + 0.05\lambda} \tag{2}$$

where $(1 + 0.05\lambda)$ is the cost division factor, with $\lambda \in \{0, 1, \ldots, 20\}$. A sensitivity analysis of the WACC's influence will also be performed. We will first assume a WACC equal to 0%. As the mean WACC for utilities in energy in the US is around 7% according to [28], we will generate results for WACC of 3.5, 7 and 10% to understand the impact of better or worse financing conditions on the viability of the project.

The link between the annualised CAPEX and the CAPEX of a technology can be written as

$$\text{CAPEX}_{\text{an}}(w) = \frac{\text{CAPEX} \cdot w}{1 - (1 + w)^{-L}}$$

where CAPEX_{an} is the annualised CAPEX of the technology, w the WACC and L its lifetime in year.[4]

In the first configuration, we only allow the installation of hydrokinetic turbines (HKT) and batteries to supply the local electricity demand. In the second configuration, we allow the possibility of adding other technologies for generating electricity. Solar PV and offshore wind turbine capacities may be deployed in addition to or in place of HKT if they result in an even lower value of the yearly costs. We rely on reanalysis data [29, 30] for the solar PV and offshore wind turbines capacity factor time series obtained from the Renewable Ninja website[5] and provided in Figures 10 and 11, respectively.

3.3 Assumptions & presentation of the second energy system

In this second energy system, we assume a factory located near the sea or ocean. The factory features a local power electricity demand displayed in Figure 13, obtained from the ELMAS dataset [31] and adapted to the year 2019. The yearly electricity consumption is chosen to match the order of magnitude of the demand of a typical factory manufacturing parts (e.g., mechanical parts for the automotive industry). Further information related to this demand curve can be found in Appendix A. The factory is connected to the mainland grid and can therefore buy or sell electricity to the market. The injection price, i.e., the price that the seller received for selling its electricity, follows the day-ahead market price corresponding to the French bidding zone for the year 2019.[6] Moreover, the factory can purchase electricity from the grid at a price equal to the day-ahead market price plus a €0.02 fee per kWh. This €0.02 surplus includes the network fees and the margin of the retailer, see Appendix A for more details. These two price time series are displayed in Figure 14. We also arbitrarily assume a €25m maximum installation budget to install electricity production and storage capacities. We will also make the assumption that obtaining a permit to install both onshore and offshore wind turbines is too constraining and time-consuming for the factory. Therefore, these technologies will be excluded from the set of alternatives to generate electricity. The optimisation objective is to satisfy the electricity demand while minimising the annualised CAPEX and OPEX, plus the expenses incurred by consuming electricity from the grid, minus the profit made by selling electricity to the grid. A study on the impact of HKT cost reduction on the results will also be carried out, in the same way as it was carried in the first energy system, following Equations (1) and (2). A sensitivity analysis will be performed on the WACC in the same way as in the first energy system.

In the first configuration, we only allow the installation of HKT and batteries. The tidal capacity factor is the same as the one applied in the island energy systems. Further information can be found in Appendix A. In the second configuration, we allow for the possibility of the factory also relying on solar PV for generating electricity. The corresponding capacity factor time series for the year 2019 is plotted in Figure 10.

3.4 Assumptions & presentation of the third energy system

In this last system, we consider the situation of an energy producer who may install HKT in order to maximise profitability by selling electricity on the day-ahead market. This producer can also deploy battery storage capacities. The sum of CAPEX value for installed capacities must remain below a given maximum budget. Electricity is sold at the same price times series as in the factory case. This time series is plotted in Figure 14. The HKT capacity factor time series is displayed in Figure 9; it remains the same as in the two other cases.

[4] We note that $\lim_{w \to 0} \text{CAPEX}_{\text{an}}(w) = \text{CAPEX}/L$. This result can be obtained with L'Hospital's rule.

[5] `https://www.renewables.ninja/`

[6] Found on the Ember website: `https://ember-energy.org/data/european-wholesale-electricity-price-data/`

4 Results

Results related to the three energy systems presented in Section 3 are briefly discussed in the next three subsections.

4.1 First system results

The first energy system features an isolated off-grid island with a demand that has to be served locally. Two configurations are envisaged. The first one (system 1.1) only allows for the installation of HKT and batteries to supply the demand. The second one (system 1.2) allows for the installation of HKT, solar PV, wind offshore turbines and batteries to supply the same demand. The results related to the first configuration show that the optimal solution obtained by optimising the model objective corresponds to €0.231m, which represents the annual expenses for covering the electricity demand of the island. To meet the demand, the associated optimal configuration includes the deployment of 780.16 kW of HKT capacity and 1260.65 kWh of battery storage capacity. By dividing the annual expenses by the annual electricity demand, we obtain an estimation of the electricity cost:

$$\frac{€0.231 \cdot 10^6}{2.6592 \cdot 10^6 \text{ kWh}} \approx €0.087/\text{kWh}.$$

The HKT cost reduction study, on this first configuration, shows a decrease in the yearly expenses, as can be seen in Figure 1.

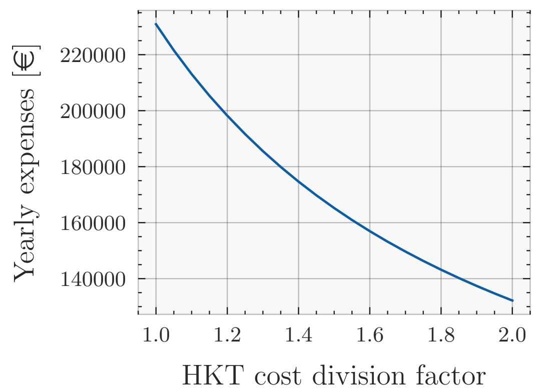

Figure 1: Evolution of the yearly expenses as a function of the HKT cost division factor - system 1.1.

We also observe a decrease in the battery storage installed capacity and, simultaneously, an increase in the HKT installed capacity, as presented in Figure 2. This decrease could be explained by the fact that, as HKT cost decrease, it becomes more profitable to increase the generation of electricity. This allows for decreasing the necessary battery storage capacity to serve all the demand, even if this leads to curtailing more electricity.

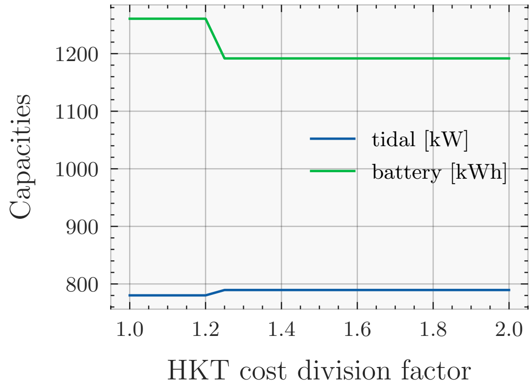

Figure 2: Evolution of the HKT and battery installed capacities as a function of the HKT cost division factor - system 1.1.

Results related to the influence of the WACC are reported in Table 1.

WACC (%)	0	3.5	7	10
HKT cap. (kW)	780.16	780.16	780.16	780.16
Battery cap. (kWh)	1260.65	1260.65	1260.65	1260.65
Elec. cost (€/kWh)	0.087	0.110	0.138	0.164

Table 1: Influence of the WACC on the installed HKT and battery capacities and on the electricity cost - system 1.1.

We observe that the WACC has no impact on the installed capacities. This could be explained by the fact that the demand has to be met, regardless of the electricity cost. In the second configuration, we obtain a yearly cost of €0.231m, which is the same value as the one obtained in the first configuration. This is explained by the fact that even if we authorise the use of solar PV and offshore wind turbines to better optimise the system, it results in installing HKT and batteries only. Note that HKT has the biggest annual costs, which are defined as the sum of annualised CAPEX and OPEX. More specifically we observe a cost of $\simeq$€251/kW/year for HKT and a cost of $\simeq$€137/kW/year for offshore wind turbines and $\simeq$€35/kW/year for solar PV.[7] On the other hand, the mean capacity factor is higher for HKT (≈ 0.59) than for offshore wind turbines (≈ 0.52) and solar PV (≈ 0.15). Let us suppose

$$\text{index} = \frac{\text{mean capacity factor}}{\text{annual costs}}$$

The index classifies the technologies in terms of mean capacity factor (MCF) per annual costs (AC); the higher it is, the better the technology is.

[7] Both solar PV and wind turbine costs come from `https://ens.dk/`

Tech.	MCF	AC	index
HKT	0.59	251	0.0024
Offshore wind turbines	0.52	137	0.0038
Solar PV	0.15	35	0.0043

Table 2: The mean capacity factor over cost index value.

In these terms, solar PV seems to have an advantage both over wind turbines and HKT. However, neither solar PV nor offshore wind turbine capacities are deployed in the optimised configuration. This could be explained by the regularity of the tide, which allows one to avoid problems associated with the *dunkelflaute* phenomenon [10].

The costs reduction study shows, similar to what was observed in the first configuration, that the value of the overall yearly costs decreases, in conjunction with a decrease in the battery storage installed capacity and, simultaneously, an increase in the HKT installed capacity. Results related to the WACC sensitivity analysis are reported in Table 3.

WACC (%)	0	3.5	7	10
HKT cap. (kW)	780.16	780.16	780.16	780.16
Battery cap. (kWh)	1260.65	1260.65	1260.65	1260.65
PV cap. (kW)	0	0	0	0
Wind cap. (kW)	0	0	0	0
Elec. cost (€/kWh)	0.087	0.110	0.138	0.164

Table 3: Influence of the WACC on the installed HKT, solar PV, wind offshore turbines and battery capacities and on the electricity cost - system 1.2.

Results for system 1.2 demonstrate that HKT is a suitable option for off-grid systems, whatever the WACC value investigated.

4.2 Second system results

The second energy system features an on-grid factory located near the seaside, with a local demand that needs to be served. Two configurations are examined. In both of them, the connection with the grid allows the factory to buy or sell energy to the grid. The first one (system 2.1) only allows for the installation of HKT and batteries to supply the demand. The second one (system 2.2) allows for the installation of HKT, solar PV and batteries to supply the same demand. The results related to the first configuration show that the value of the optimisation objective, i.e. the yearly electrical expenses minus the yearly electrical profit, is €3.44m. This optimal solution is obtained by installing 7.35MW HKT capacity and no battery. A total of 27.69 GWh is consumed from the grid, costing €1.712m, while 3.50 GWh is injected into the grid, giving back €0.117m. The behaviour of the system on a typical week can be found in Figure 4.

We can compute an approximation of the cost of electricity by dividing the total annual costs by the annual electricity demand:

$$\frac{€3.44 \cdot 10^6}{61.9166 \cdot 10^6 \text{kWh}} = €0.056/\text{kWh}.$$

Without the installation of HKT, the only way to serve the electricity demand would be to buy all the electricity from the grid and possibly install batteries. Results show that this would lead to an electricity cost of €0.061/kWh, without batteries. Therefore, the savings associated with the installation of HKT are €0.005/kWh, with the current HKT cost.

As the HKT cost decreases, we observe a decrease in the objective value coupled with a decrease in the expenses associated with electricity purchased from the grid. Revenues associated with the injection of electricity on the grid also grow, as shown in the Figure 3.

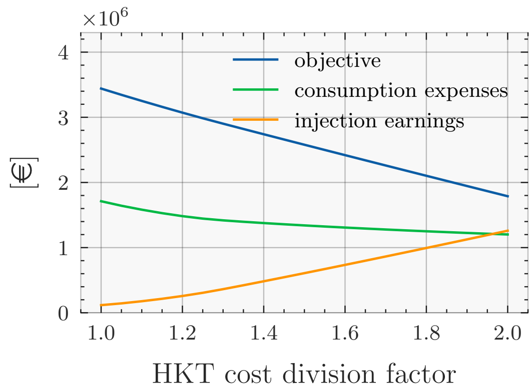

Figure 3: Evolution of the overall cost, the consumption from the grid and the injection earnings as a function of the decrease of the CAPEX and OPEX of HKT - system 2.1.

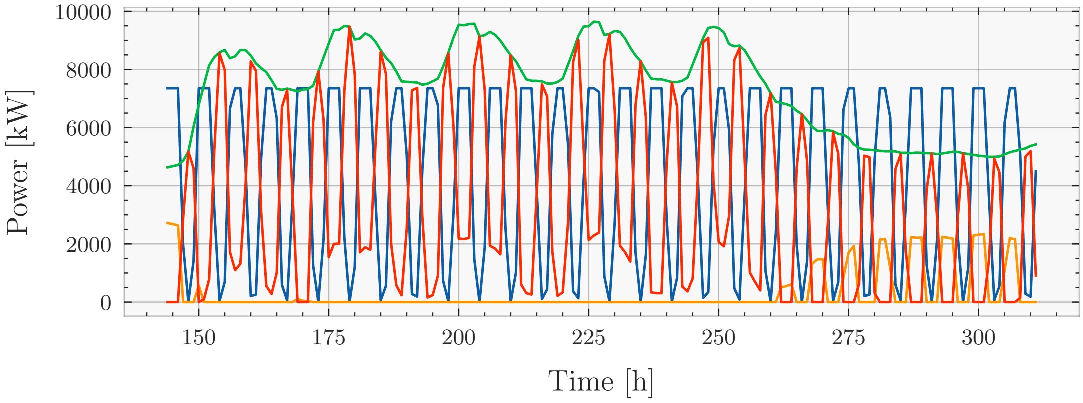

Figure 4: Graphical illustration of a typical behaviour of the system during a winter week showing the power produced by HKT in blue, the demand curve in green, the consumption from the grid in red and the injection into the grid in orange - system 2.1.

Regarding installed capacities, the HKT installed capacity grows while the battery storage installed capacity remains at 0kWh, as shown in the Figure 5.

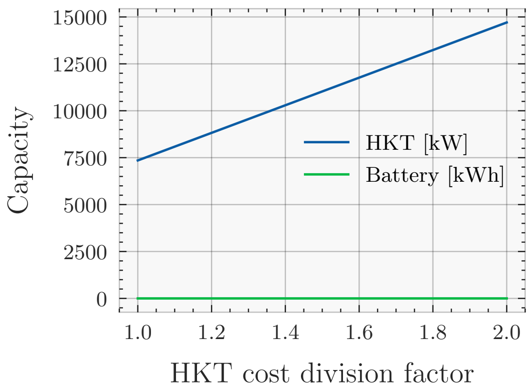

Figure 5: Evolution of the installed capacities for HKT and battery storage as a function of the HKT overall yearly costs decrease - system 2.1.

Results related to the WACC sensitivity analysis are reported in Table 4.

WACC (%)	0	3.5	7	10
HKT cap. (kW)	7352.94	0	0	0
Battery cap. (kWh)	0	0	0	0
Demand (GWh)	61.92	61.92	61.92	61.92
Inj. earn. (€m)	0.12	0	0	0
Consu. costs (€m)	1.71	3.77	3.77	3.77
Elec. cost (€/kWh)	0.056	0.061	0.061	0.061

Table 4: Influence of the WACC on the installed HKT, solar PV and battery capacities, on the injection earnings, the consumption expenses and electricity cost - System 2.1.

We observe the impact that the WACC can have on the systems. In the first configuration, with a 3.5% WACC, leading to an annualised HKT CAPEX of €220.84, the optimal solution not longer includes any HKT. Buying electricity from the grid is thus cheaper than installing HKT. In the second configuration, the optimal solution has an objective value (i.e. the yearly electrical expenses minus the yearly electrical profit) of €2.94m, associated with a 28.74MW solar PV capacity, no HKT nor battery. A total of 39.87GWh is purchased from the grid over a year, costing €2.45m, while 15.73GWh is injected into the grid, providing a revenue of €0.54m. By dividing the value of the optimisation objective by the annual electricity demand, we obtain an estimation of the cost of electricity:

$$\frac{€2.94 \cdot 10^6}{61.9166 \cdot 10^6 \text{kWh}} = €0.047/\text{kWh}.$$

The typical behaviour of system 2.2 on a summer week is displayed in Figure 8, showing the evolution of solar PV production, electricity demand, purchase and injection on the grid. Depending on the cost decrease, three distinct phases can be identified:

1. In the first phase, the system is only exploiting solar resources. The objective value, the solar PV capacity, the consumption and the injection remain the same.

2. In the second phase, the system becomes hybrid, using both HKT and solar PV technologies. The value of the optimisation objective decreases. We first observe a drop in the injection of electricity, due to the decrease in solar PV capacity. This solar PV capacity decrease can be explained by the fact that HKT electricity production becomes more competitive, while being intrinsically more regular than solar PV production. The system uses the electricity generated by the HKT to supply the demand, reducing the injection. In the same way, consumption from the grid also decreases. We then observe a slight increase in the injection of electricity into the grid,

explained by the fact that the installed HKT capacity increased, leading to a higher electricity production. The volume of electricity that is not consumed locally is also increasing and is thus injected into the grid.

3. In the third phase, the system only relies on HKT. The injection of electricity into the grid increases while the objective and the amount of electricity consumed from the grid decrease.

Figure 6 and 7 show the evolution of the capacities and the costs with the HKT cost reduction.

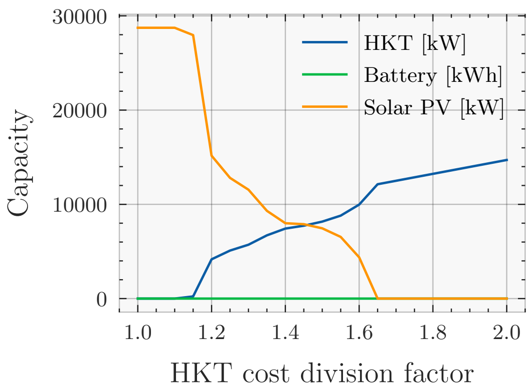

Figure 6: Evolution of the installed capacities of HKT, solar PV and battery storage as a function of the decrease of the CAPEX and OPEX of HKT - system 2.2.

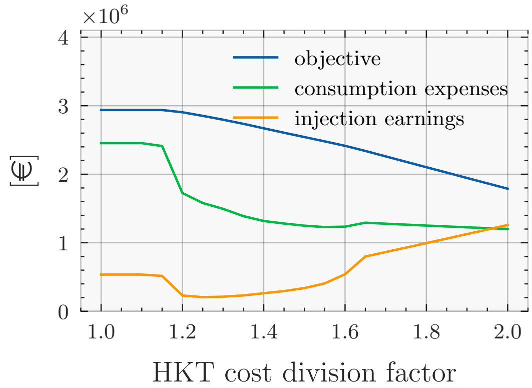

Figure 7: Evolution of the overall costs, the purchase of electricity from the grid, and the injection earnings as a function of the decrease of the overall yearly cost of HKT - system 2.2.

Results related to the WACC sensitivity analysis are reported in Table 5.

WACC (%)	0	3.5	7	10
HKT cap. (kW)	0	0	0	0
Battery cap. (kWh)	0	0	0	0
PV cap. (kW)	28735.63	26660.44	0	0
Inj. earn. (€m)	0.54	0.46	0	0
Consu. costs (€m)	2.45	2.49	3.77	3.77
Elec. cost (€/kWh)	0.047	0.056	0.061	0.061

Table 5: Influence of the WACC on the installed HKT, solar PV and battery capacities, on the injection earnings, the consumption expenses and electricity cost - system 2.2.

The phenomenon observed in the first configuration (system 2.1) is also present here, but with solar PV.

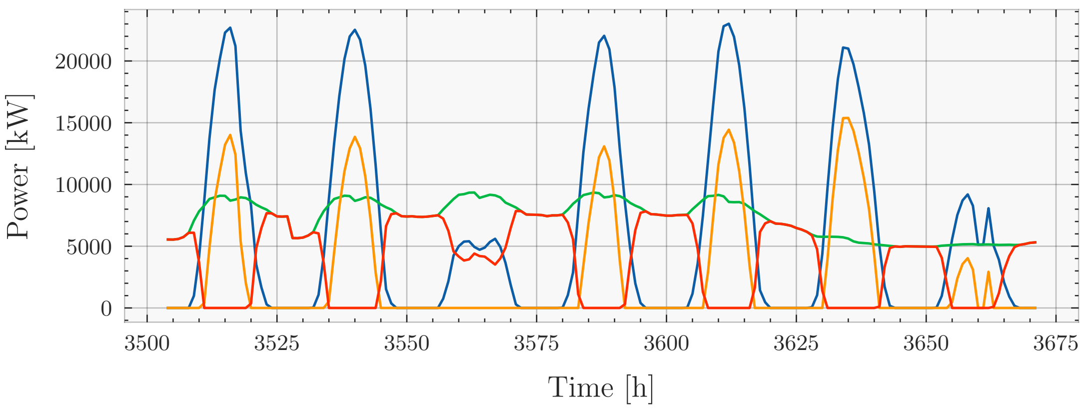

Figure 8: Graphical illustration of a typical behaviour of the system during a summer week showing the power produced by solar PV in blue, the demand curve in green, the injection into the grid in orange and the consumption from the grid in red - system 2.2.

4.3 Third system results

The third energy system features an energy producer whose goal is to maximise the profit made by selling electricity produced by HKT on the day-ahead market. Results related to this third energy system show that it is not profitable to install hydrokinetic turbines. Since no investments are made, the expenses and revenues are thus equal to 0.

Results of the cost reduction study show that when the HKT cost are divided by ≈ 1.25, it becomes profitable to produce electricity with HKT and sell it on the day-ahead market. The profit then increases as a function of the dividing factor.

We did not analyse the influence of the WACC on the third configuration because it was already determined as unprofitable with a 0% WACC.

5 Discussion of the results

As synthesised in Table 6, our results show that there is potential in investing in HKT when a local demand needs to be served. The potential is greater when there is no grid connection, as is the case in the first system. In the second configuration of this first system, with assumed costs, HKT represent the optimal option to meet the demand, even if we could install solar PV or offshore wind turbines that are cheaper. When we have a grid connection and a local demand that needs to be met with the possibility to install HKT and solar PV (system 2.2), HKTs appear when their costs are reduced. It creates, at first, a hybrid system where solar PV and HKT are installed. Afterwards, solar PV tends to disappear when HKT costs are further reduced. However, when it comes to producing electricity to sell to the day-ahead market, HKT is not yet a viable option. This means that investing in HKT for this purpose results in a financial loss. We did not assess the potential revenues of HKT in other markets, such as capacity markets.

The WACC sensitivity analysis shows us that in the first energy system (first and second configurations), the WACC has no impact on the installed capacities. Results for system 1.2 demonstrate that HKT is a suitable option for off-grid systems, whatever the WACC value investigated. In the second energy system, we observe the impact that the WACC can have on the systems. In the first configuration, with a 3.5% WACC, leading to an annualised CAPEX of €220.84, the optimal solution no longer includes any HKT. Buying electricity from the grid is thus cheaper than installing HKT. In system 2.2, the same phenomenon is observed with solar PV.

6 Conclusion

In this paper, we analysed three energy systems related to hydrokinetic energy (an off-grid island, an on-grid factory and an electricity producer). The objectives of this analysis were: (i) to observe whether hydrokinetic energy may be an economically viable solution to produce electricity, and (ii) to determine the resulting costs of electricity. A study on the influence of HKT cost has also been conducted for each energy system. Our results show that even with high installation and maintenance costs, HKT represent the optimal option compared to offshore wind turbines or solar PV when an off-grid local electricity demand has to be served, such as in the first energy system configurations. When a local demand has to be served with a connection to the grid, HKT are being installed to complement solar PV capacities as their cost decreases, thus showing a synergy PV-HKT that allows for reducing the amount of electricity purchased from the grid. Based on the assumed installation and maintenance costs, HKT does not seem to be profitable for an electrical producer that would like to sell the generated electricity on the day-ahead market.

One needs to remember that the computation of the electricity costs rely on input data for techno-economic parameters and time series (e.g., tidal, solar PV, wind turbine production, demand, market prices). The quality of these data has a strong influence on the output results. In this paper, we have partially relied on synthetic data for the HKT capacity factor time series.

In this respect, we suggest as a first research direction, collecting real-life data related to hydrokinetic electricity energy generation time series. Having a better knowledge of these time series would certainly improve the accuracy of the results we could obtain for the three energy systems considered. We note that these time series are location dependent.

As a second future direction, we aim to conduct a systematic review of locations where the introduction of HKT would be profitable, with an emphasis on islandic systems. To carry out this identification, it would be appropriate to first analyse the features that characterise promising candidate systems. Several promising islands have already been identified in France as being good candidates to deploy HKT turbines in cooperation with other renewable energy production capacities and battery storage, such as, for instance, the Ouessant island, where a microgrid is being progressively deployed, featuring HKT, solar PV, wind turbines, storage capacities, and dynamic off-peak hours system.[8]

As a third research direction, we would like to focus on identifying, based on the potential sites, the most desirable features of HKT (e.g., power, size, power

[8] https://www.cre.fr/documents/fiches-demonstrateurs-smartgrids/ile-douessant.html

System	1.1	1.2	2.1	2.2	3
HKT capacity (kW)	780.16	780.16	7352.94	0	0
Battery capacity (kWh)	1260.65	1260.65	0	0	0
Solar PV capacity (kW)	-	0	-	28735.63	-
Wind offshore turbine capacity (kW)	-	0	-	-	-
Yearly demand (GWh)	2.66	2.66	61.92	61.92	-
Installation budget (€m)	-	-	25	25	10
Injection earnings (€m)	-	-	0.12	0.54	0
Consumption costs (€m)	-	-	1.71	2.45	-
Electricity cost (€/kWh)	0.087	0.087	0.056	0.047	-

Table 6: Synthesis of the results found by our study.

curve characteristics), in order to guide future mechanical developments. This would depend on several factors, like the power to be provided, availability of the resources, environmental constraints (e.g., leading to a very low mortality of fish), maintenance costs, etc.

Acknowledgements

This work has been prepared with the support of the European Union in the context of the Interreg North-West Europe SHINES project (`https://shines.nweurope.eu/`). Victor Dachet gratefully acknowledges the financial support of the Wallonia-Brussels Federation for his FRIA grant. We also thank Marcel Thos for scientific discussions in the early stage of this project.

References

[1] A. Kumar, S. Nagar, and S. Anand. 1 - Climate change and existential threats. In Suruchi Singh, Pardeep Singh, S. Rangabhashiyam, and K.K. Srivastava, editors, *Global Climate Change*, pages 1–31. Elsevier, 2021. ISBN 978-0-12-822928-6.

[2] M.K.G. Deshmukh, M. Sameeroddin, D. Abdul, and M.A. Sattar. Renewable energy in the 21st century: A review. *Materials Today: Proceedings*, 80:1756–1759, 2023.

[3] M. Roser. Learning curves: What does it mean for a technology to follow Wright's Law? *Our World in Data*, 2023.

[4] A Elia, M. Taylor, B. Gallachóir, and F. Rogan. Wind turbine cost reduction: A detailed bottom-up analysis of innovation drivers. *Energy Policy*, 147:111912, 2020.

[5] L. Susskind, J. Chun, A. Gant, C. Hodgkins, J. Cohen, and S. Lohmar. Sources of opposition to renewable energy projects in the United States. *Energy Policy*, 165:112922, 2022.

[6] G.S. Nieminen and E. Laitinen. Understanding local opposition to renewable energy projects in the Nordic countries: A systematic literature review. *Energy Research & Social Science*, 122: 103995, 2025.

[7] C.R. Jones and J.R. Eiser. Understanding 'local' opposition to wind development in the UK: how big is a backyard? *Energy policy*, 38(6):3106–3117, 2010.

[8] S. Impram, S.V. Nese, and B. Oral. Challenges of renewable energy penetration on power system flexibility: A survey. *Energy strategy reviews*, 31: 100539, 2020.

[9] M. Berger, D. Radu, R. Fonteneau, R. Henry, M. Glavic, X. Fettweis, M. Le Du, P. Panciatici, L. Balea, and D. Ernst. Critical time windows for renewable resource complementarity assessment. *Energy*, 198:117308, 2020.

[10] B. Li, S. Basu, S.J. Watson, and H.W.J. Russchenberg. A brief climatology of Dunkelflaute events over and surrounding the North and Baltic Sea areas. *Energies*, 14(20):6508, 2021.

[11] T. Ghanbarzadeh, D. Habibi, S.M. Uddin, and A. Aziz. Generation expansion planning: Transitioning toward decarbonization with a focus on reliability and Dunkelflaute. *Electric Power Systems Research*, 248:111871, 2025.

[12] W.I. Ibrahim, M.R. Mohamed, R.M.T.R. Ismail, P.K. Leung, W.W. Xing, and A.A. Shah. Hydrokinetic energy harnessing technologies: A review. *Energy Reports*, 7:2021–2042, 2021. ISSN 2352-4847.

[13] V. Dachet, A. Dubois, B. Miftari, R. Fonteneau, and D. Ernst. Remote Renewable Energy Hubs: A taxonomy. *Energy Reports*, 13:3112–3120, 2025.

[14] M. Berger, D. Radu, G. Detienne, T. Deschuyteneer, A. Richel, and D. Ernst. Remote renewable

hubs for carbon-neutral synthetic fuel production. *Frontiers in Energy Research*, 9:671279, 2021.

[15] V. Dachet, A. Maio, P. Counotte, R. Fonteneau, and D. Ernst. Remote Renewable Energy Hubs in the High Seas Using Batteries as Energy Vector. E-print, 02 May 2025.

[16] B. Miftari, M. Berger, H. Djelassi, and D. Ernst. GBOML: Graph-based optimization modeling language. *Journal of Open Source Software*, 7(72): 4158, 2022.

[17] A. Larbanois, B. Miftari, A. Mouchamps, Ayyildiz Kerem Enes, V. Schryvers, G. Derval, and D. Ernst. Lead-cooled fast reactor SMR integration: An off grid study case based on a real-life demand. E-print, 28 July 2025.

[18] J. Mbenoun, A. Benzerga, B. Miftari, G. Detienne, T. Deschuyteneer, J. Vazquez, G. Derval, and D. Ernst. Integration of offshore energy into national energy system: A case study on Belgium. *Applied Energy*, 382:125031, 2025.

[19] C. Shetty and A. Priyam. A review on tidal energy technologies. *Materials Today: Proceedings*, 56:2774–2779, 2022. 3rd International Conference on Contemporary Advances in Mechanical Engineering.

[20] J.F. Bárcenas Graniel, J.V.H. Fontes, H.F.G. Garcia, and R. Silva. Assessing hydrokinetic energy in the Mexican Caribbean: A case study in the Cozumel channel. *Energies*, 14(15):4411, 2021.

[21] M. A. Almoghayer, D. K. Woolf, S. Kerr, and G. Davies. Integration of tidal energy into an island energy system – A case study of Orkney islands. *Energy*, 242:122547, 2022.

[22] P. Garcia-Novo, D. Coles, Y. Kyozuka, R. Yamada, H. Moriguchi, and D. Sakaguchi. Optimization of a tidal–wind–solar system to enhance supply–demand balancing and security: A case study of the Goto Islands, Japan. *Sustainability*, 15(12):9147, 2023.

[23] J.B. Johnson and D.J. Pride. River, tidal, and ocean current hydrokinetic energy technologies: Status and future opportunities in Alaska. *Prepared for Alaska Center for Energy and Power*, 2010.

[24] G.R. Ileberi and P. Li. Integrating hydrokinetic energy into hybrid renewable energy system: Optimal design and comparative analysis. *Energies*, 16(8):3403, 2023.

[25] D. Khojasteh, D. Khojasteh, R. Kamali, A. Beyene, and G. Iglesias. Assessment of renewable energy resources in Iran; with a focus on wave and tidal energy. *Renewable and Sustainable Energy Reviews*, 81:2992–3005, 2018.

[26] D.M. Fouz, R. Carballo, V. Ramos, and G. Iglesias. Hydrokinetic energy exploitation under combined river and tidal flow. *Renewable Energy*, 143: 558–568, 2019.

[27] Gurobi Optimization, LLC. Gurobi Optimizer Reference Manual, 2024. URL `https://www.gurobi.com`.

[28] Aswath Damodaran. Cost of Capital by sector (US), 2024. URL `https://pages.stern.nyu.edu/~adamodar/New_Home_Page/datafile/wacc.html`. Accessed: 2025-06-10.

[29] S. Pfenninger and I. Staffell. Long-term patterns of European PV output using 30 years of validated hourly reanalysis and satellite data. *Energy*, 114: 1251–1265, 2016.

[30] I. Staffell and S. Pfenninger. Using bias-corrected reanalysis to simulate current and future wind power output. *Energy*, 114:1224–1239, 2016.

[31] K. Bellinguer, R. Girard, A. Bocquet, and A. Chevalier. ELMAS dataset. 9 2023.

A Appendix

A.1 Parameters

Table 7 summarises most of the parameters used in the experiments.

Parameter	Reference value	Parameter	Reference value
HKT CAPEX	€3400/kW	HKT OPEX	€100/kW/year
HKT lifetime	22.5 years		
Solar PV CAPEX	€870/kW	Solar PV OPEX	€10.6/kW/year
Solar PV lifetime	35 years		
Wind offshore turbine CAPEX	€2780/kW	Wind offshore turbine OPEX	€44/kW/year
Wind offshore turbine lifetime	30 years		
Battery CAPEX	€290/kWh	Battery OPEX	€8.4/kWh/year
Battery lifetime	15 year		

Table 7: Values of techno-economic parameters considered in this paper. Values are taken from OceanSET Third Annual Report for HKT parameters, and from the ens.dk website for other values.

A.2 Capacity factors

In this article, we rely on a simplified synthetic capacity factor time series for the HKT. It is generated using the following equation:

$$\forall t \in \{0, 8760-1\}, f(t) = \min\left\{1, \left|k * \sin\left(\frac{2\pi t}{T}\right)\right|^3\right\} \tag{3}$$

with $T = 12.4215$ and $k > 0$. To obtain this curve, we make the following assumptions:

- We assume that the streamflow velocity is a sinus function of the time with periodicity T, where T corresponds to the periodicity of the tide (in hours). The influence of a full moon and new moon, as well as the role of equinoxes, is left for future work.
- As the theoretical power output of HKT mainly depends cubically on the streamflow velocity, we consider a cubic function of the velocity as the theoretical time-dependent power density;
- The min operator is used to transform the theoretical power density time series into a capacity factor time series. It models the rated velocity of the wind turbine by setting a plateau to 1 as soon as the velocity is above a given threshold. This threshold is implicitly defined using the k parameter.

As a consequence, the parameter k also enables tuning of the average capacity factor. A value of $k = 1$ provides a 42,4% average capacity factor, while a value of $k = 2$ provides a value of 58,6 % average capacity factor. A plot of the first values of the capacity factor time series corresponding to $k = 2$ is provided in figure 9.

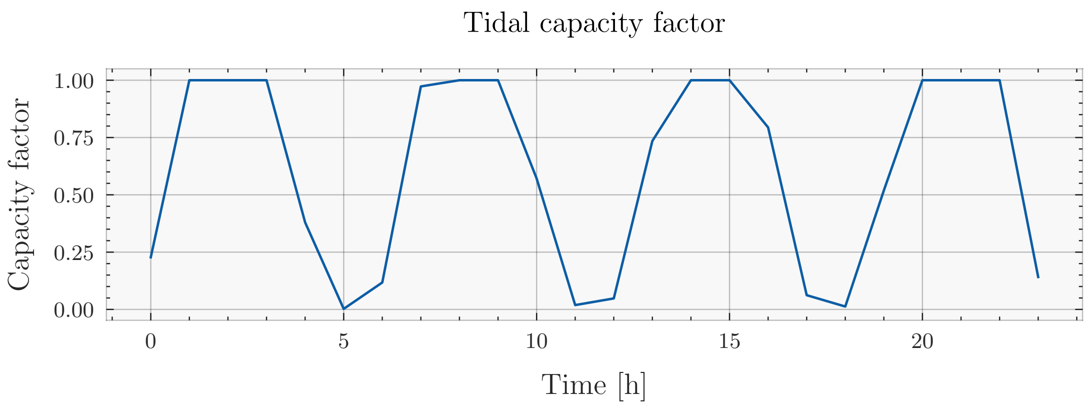

Figure 9: Illustration of the HKT synthetic capacity factor time series.

The capacity time series related to solar PV and offshore wind production, obtained from the Renewable Ninja portal[29, 30], are displayed in Figure 10 and 11.

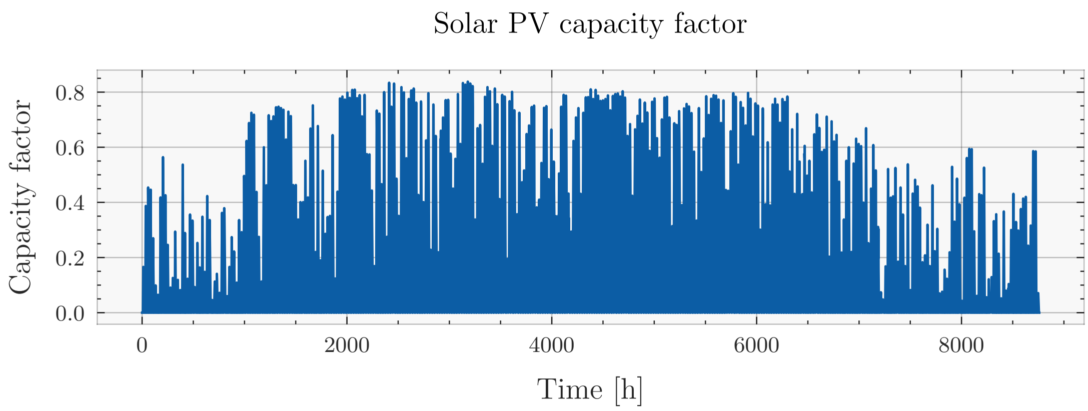

Figure 10: Capacity factor times series for solar PV production for the Paimpol-Bréhat location, obtained from the Renewable Ninja website, year 2019.

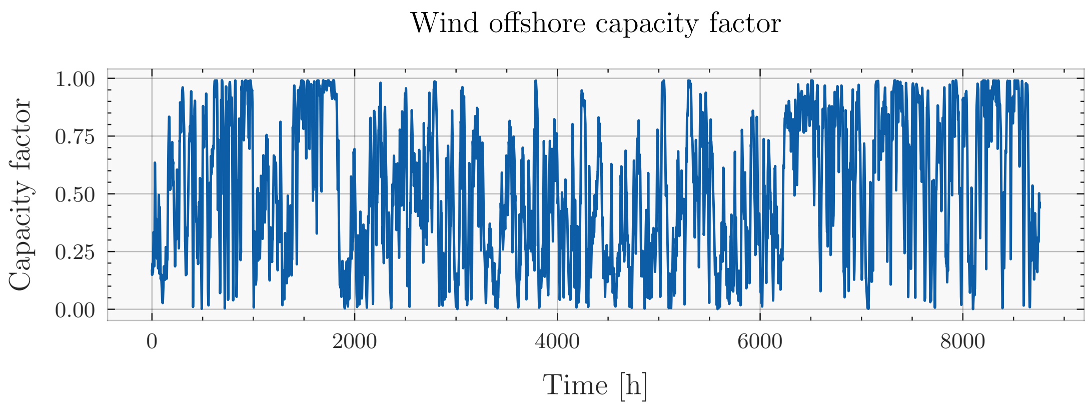

Figure 11: Capacity factor times series for offshore wind production for the Paimpol-Bréhat location, obtained from the Renewable Ninja website, year 2019.

A.3 Demand curves

The electricity demands considered in the various systems are displayed in Figure 12 and 13.

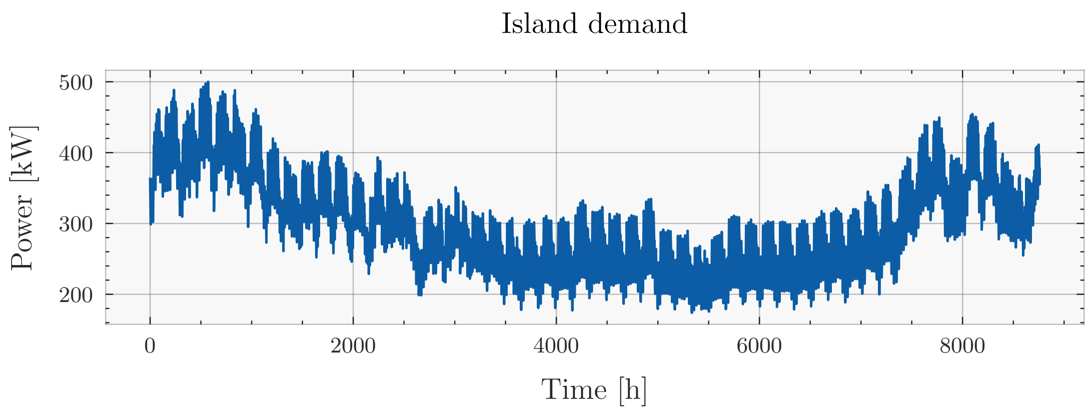

Figure 12: Electricity demand for systems 1.1 and 1.2.

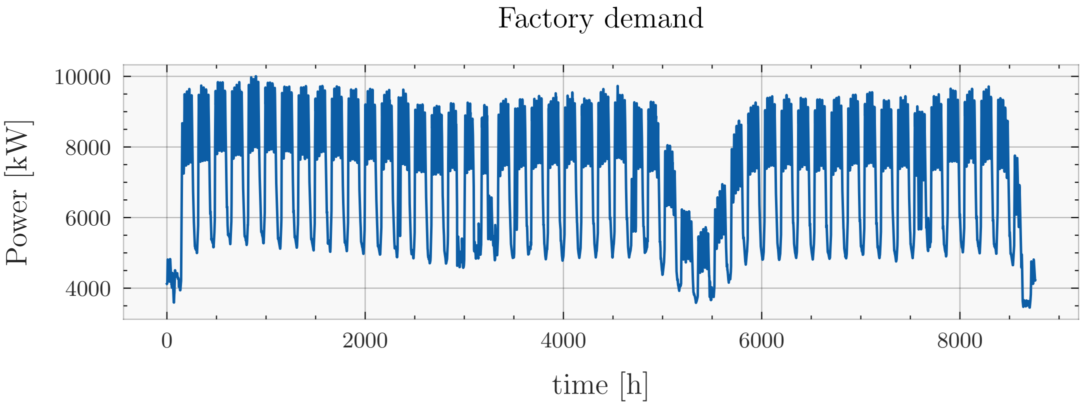

Figure 13: Electricity demand for subsystems 2.1 and 2.2.

The island is supposed to have a population of roughly 1,200 inhabitants, consuming 2,223 kWh per year, corresponding to the average electricity consumption of a mainland France resident.[9] To generate the hourly Island demand curve, we normalised data from the RTE website[10] and multiplied them by 500 to have a yearly consumption of

$$\sum_{t=0}^{T-1} P_t^{\mathrm{L}} \cdot \Delta t \approx 2.659242 \text{ GWh},$$

precisely representing the consumption of 1196.24 inhabitants, with the previous assumptions. P_t^{L} is the hourly electrical load in kW, assumed to be constant during hour $t \in \{0 \dots T-1\}$ with $T = 8760$ corresponding to the number of hours in a year and $\Delta t = 1$ representing an hourly resolution.

Concerning the factory demand, we use the same methodology as for the island case. The yearly electricity consumption is chosen to match the order of magnitude corresponding to the demand of a typical factory manufacturing parts (e.g., mechanical parts for the automotive industry). The initial hourly power demand curve was found on the ELMAS dataset [31], normalised, adapted to suit the 2019 calendar and multiplied by 10000, which is an arbitrary choice. The demand over a year can be computed as follows:

$$\sum_{t=0}^{T-1} P_t^{\mathrm{L}} \cdot \Delta t \approx 61.9166 \text{ GWh},$$

where P_t^{L} is the hourly electrical power load in kW assumed to be constant during hour $t \in \{0, T-1\}$ with $T = 8760$ corresponding to the number of hours in a year and $\Delta t = 1$ representing an hourly resolution. The factory shows a lower power demand during weekends and holidays than during weekdays. We also observe a decrease in the power demand during the night.

A.4 Electricity costs

In this article, we rely on the day-ahead market price time series corresponding to the French bidding zone for the year 2019. It corresponds to the blue curve in Figure 14. The green curve corresponds to the purchase tariff, obtained by adding €0.02/ kWh to the day-ahead market price. This €0.02 fee corresponds to the network fees and the retailer margin. More specifically, to determine this value of €0.02/kWh, we have considered a network fee of c€1.96/kWh to which we have added a c€0.04/kWh retailer margin. We note that this network fee is typical of the network fee paid in France by a customer connected to the HTA voltage (typically 20kV), as can be computed from the Enedis report.[11]

[9] `https://www.data.gouv.fr/reuses/consommation-par-habitant-et-par-ville-delectricite-en-france/`

[10] `https://www.rte-france.com/eco2mix/telecharger-les-indicateurs`

[11] `https://www.france-hydro-electricite.fr/wp-content/uploads/2019/09/TURPE_5bis_plaquette_tarifaire_aout_2019.pdf`

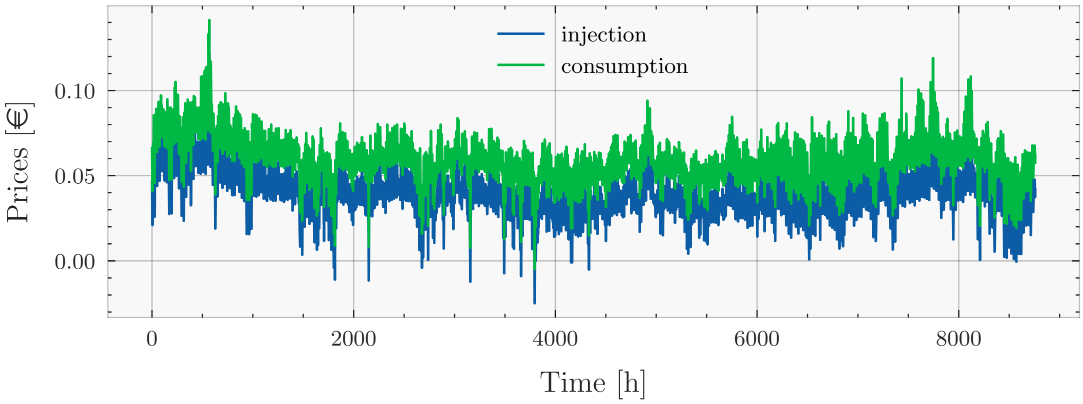

Figure 14: Electricity price time series for purchase and injection.